Supplementary Information:

# Manganese-enriched $CsPbCl_3$ perovskite nanocrystals for self-assembled supercrystals

*Victoria Lapointe,*[a] *Marek B. Majewski* [a*]

[a] *Department of Chemistry and Biochemistry and Centre for NanoScience Research Concordia University 7141 Sherbrooke Street West, Montreal, Quebec, Canada, H4B 1R6*

*E-mail: marek.majewski@concordia.ca

# Table of Contents

## Experimental Methods

### Materials

All chemicals were used as received from commercial sources: $Cs_2CO_3$ (Alfa Aesar), $PbCl_2$ (Baker), $MnCl_2$ (97%, Acros Organics), oleic acid (OLAC, 90%, Alfa Aesar), tri-n-octylphosphine (TOP, Alfa Aesar), oleylamine (OLAM, 70%, Sigma-Aldrich), 1-octadecene (90%, Sigma-Aldrich), hexanes (98%, Sigma-Aldrich), toluene (Thermo Fisher), ethanol (95%, Thermo Fisher), acetone (Thermo Fisher), nitric acid (75%, Sigma-Adrich), silicon substrate wafers (Si Substrate, ALPHA Nanotech; grade: prime/CZ virgin, type: n /phosphorus doped, orientation: <100>, resistivity: 1 – 30 Ω cm, thickness: 300 ± 10 μm, surface: polished front and etched back).

### Synthesis and Isolation of Perovskite Nanocrystals (PNCs)

Solution A: A cesium oleate solution was prepared with $Cs_2CO_3$ (204 mg, 0.632 mmol) and OLAC (0.625 mL, 1.97 mmol) and ODE (10 mL, 31.2 mmol) in a three neck round bottom flask. This solution was heated to 100 ℃ for 1 hour in a nitrogen atmosphere and left to dissolve. The solution was then heated to 130 ℃ in a nitrogen atmosphere and 0.45 mL was used for the hot injection.

Solution B: In a three-neck flask, $PbCl_2$ (54 mg, 0.194 mmol), OLAM (0.5 mL, 1.52 mmol), OLAC (0.5 mL, 1.58 mmol), and TOP (1 mL, 2.24 mmol) were added to ODE (5 mL, 15.6 mmol) and heated in a nitrogen atmosphere at 105 ℃ for 1 hour. In addition to these components, the manganese-doped samples had various amounts of $MnCl_2$ (10 – 30 g, 0.0795 – 0.238 mmol) added.

Hot-injection: Solution B was heated to 185 ℃ in a nitrogen atmosphere and 0.45 mL of Solution A was swiftly injected. The flask was then immediately cooled to room temperature using an ice bath. The resulting mixture turned cloudy white and was centrifuged at 12000 rpm (13400 rcf) for 10 minutes. The supernatant was discarded. The centrifuge tubes containing the pellets were left upside down to remove as much of the oily residue (unincorporated surfactants) as possible for 15 mins. The pellet was then dispersed in approximately 3-4 mL of hexanes. These colloids were stored overnight in a dark cabinet and used for further characterization or the self-assembly of SCs without further purification.

Self-assembly of PNC Supercrystals (SCs)

All doped and undoped PNC colloids were dried using a strong stream of nitrogen until no solvent remained, then were redispersed in 0.5 mL of toluene and filtered using a 2 μm PTFE filter. To induce self-assembly, 10 μL of the concentrated PNC solutions was drop cast on a 5 × 5 mm Si Substrate (previously washed with ethanol and acetone). These Si Substrates were left in a nitrogen chamber or vacuum oven to slowly evaporate the toluene overnight. The addition of tri-n-octyl phosphine (TOP) as a ligand during the hot-injection process alongside oleylamine (OLAM) and oleic acid (OLAC) rendered the PNCs oilier requiring longer drying times as compared to past work[1] to yield "dry" SCs on the silicon substrates. The as-synthesized SCs were stored in a nitrogen chamber or vacuum oven until they were needed.

Characterization

Solution UV-Vis absorbance measurements were carried out on a Cary 5000 Series UV-Vis spectrophotometer (Agilent Technologies) with a single beam range between 360 – 800 nm. The samples were diluted in a 1 cm pathlength cuvette and the baseline trace was collected using a cuvette filled with toluene.

All photoluminescence data (PL, TRPL, and PLQY) were collected using a Horiba PTI QuantaMaster 8075 Spectrofluorometer. For colloidal samples, photoluminescence data were collected at an excitation wavelength of 365 or 370 nm with an integration time of 0.5 s, step size of 2 nm, slits of 1 nm, with an automatic 5 second dark background collection and were measured in a 1 cm pathlength cuvette with hexanes or toluene as a solvent and as a blank. For solid-state samples, a quartz slide was used as the mounting substrate for the SCs on Si substrates to be mounted onto a rotating solid sample holder rotated ~30 ° relative to the incident light source. Small amounts of vacuum grease were used to keep the Si substrate in place on the quartz slide. The substrate was oriented vertically in the sample chamber, and its position was adjusted such that light from the excitation monochromator hit directly onto the SCs. Photoluminescence data of solid samples was collected at an excitation of 365 or 370 nm with an integration time of 0.5 s, a step size of 2 nm, slits of 1 nm, with an automatic 5 second dark background collection. A quartz

slide with grease and plain Si Substrate on it was used as a blank for these measurements. This same instrument equipped with an integrating sphere (Horiba K-Sphere Petit) was used for photoluminescence quantum yield measurements.

Powder X-ray diffraction (PXRD) data for the PNCs and SCs were obtained using a Rigaku Miniflex600/600C benchtop (Applied Rigaku Technologies Inc., Austin, TX, USA) equipped with CuKα X-ray source (wavelength, λ = 1.54 Å, radiation operating at 40 kV and 15 mA), a D/teX Ultra2 high=speed 1D detector or HyPix-400 MF 2D sensitive detector (Applied Rigaku Technologies Inc., Austin, TX, USA) and a nickel filter. Sample data was collected using a continuous coupled θ/2θ scan in the 2θ – range of 10 – 60 ° with step size of 0.01-0.02 ° and a scan rate between 0.5 – 1° per second. PNCs were mixed with silica particles to stop them from self-assembling on the zero-background silicon wafer sample holder while the SC Si substrates were mounted onto a sample holder with sticky tack to ensure the surface of the sample was leveled with the surface of the sample holder for measurements. Once the SL data was collected, the data was converted from ° 2θ to q-vector space using the equation $q = \frac{4\pi \sin\theta}{\lambda}$ where q is the q-vector space (Å$^{-1}$), θ is angle (radians), and λ is the X-ray source wavelength (Å). From this, the SL periodicity was estimated by fitting the 15 ° 2θ splitting to Gaussian peaks using Origin and substituting the respective peak maxima into the equation $\Lambda = \frac{2\pi}{\Delta q}$ where Δq is the distance between the fringes (Å) at 15 ° 2θ (1.06 Å$^{-1}$). The d-spacing was estimated by associating it to the center q-vector spacing between the fringes (Å) at 15 ° 2θ (1.06 Å$^{-1}$) as well.

Scanning electron microscopy (SEM) measurements were performed on a Phenom ProX G5 scanning electron microscope (Thermo Fisher Scientific). Micrographs were obtained with an acceleration voltage of 5 – 15 keV. The SCs on Si Substrates were held onto the sample holder using carbon tape. ImageJ[2] was used to calculate the average SC size using ~200 PNCs. ImageJ was used to calculate the average SC size using ~100 particles.

Transmission electron microscopy (TEM) was preformed on a Talos L120C. Micrographs were obtained with an accelerated voltage between 20-120 kV. The PNCs were diluted in hexanes by a factor of 50 before a copper TEM grid was dipped into the PNC solutions and left to dry fully to avoid any self-assembly. ImageJ[2] was used to calculate the average PNC size using ~200 particles.

Scanning Transmission electron microscopy (STEM) energy-dispersive X-ray spectroscopy (EDS) analysis were done on a Talos F200X STEM with a high-angle annular dark-field (HAADF) detector and 4 SDD Super-X detectors. Micrographs and mapping were obtained with an accelerated voltage of 200 kV. The PNCs were diluted in hexanes by a factor of 50 before a copper TEM grid was dipped into the PNC solutions and left to dry fully to avoid any self-assembly.

Inductively coupled plasma mass spectrometry (ICP-MS) analysis was done using an Agilent 7500ce (Agilent). Mn, Cs and Pb standards were mixed and diluted with 5% nitric acid. The calibration curves were established using the standard solutions at concentrations of 0, 0.05, 0.1, 1, and 10 ppm. Samples were run as individual batches after having been digested in 5% nitric acid and hydrogen peroxide before diluting to ~1ppm.

References

(1) Lapointe, V.; Green, P. B.; Chen, A. N.; Buonsanti, R.; Majewski, M. B. Long Live(d) $CsPbBr_3$ Superlattices: Colloidal Atomic Layer Deposition for Structural Stability. *Chem. Sci.* **2024**, *15* (12), 4510–4518. https://doi.org/10.1039/D3SC06662B.
(2) Schneider, C. A.; Rasband, W. S.; Eliceiri, K. W. NIH Image to ImageJ: 25 Years of Image Analysis. *Nat Methods* **2012**, *9* (7), 671–675. https://doi.org/10.1038/nmeth.2089.

Supplementary Figures

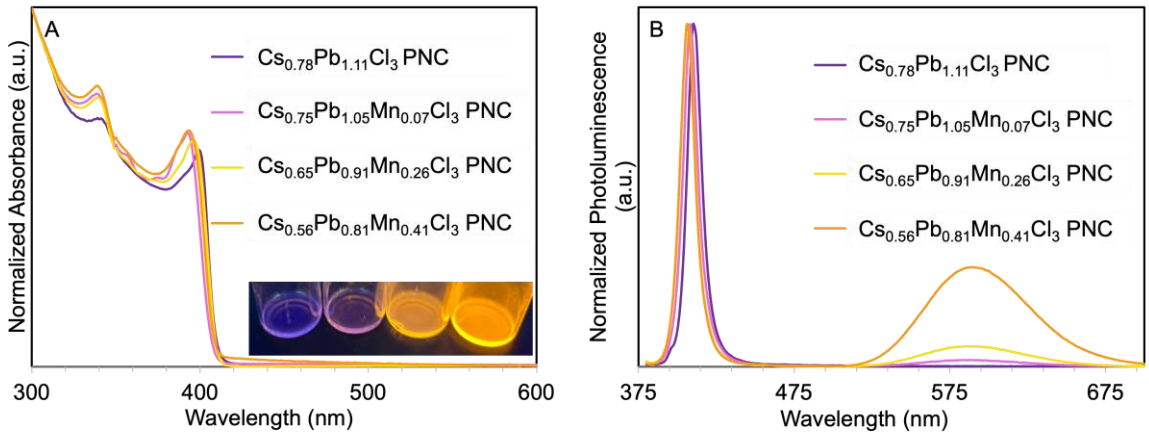


**Figure S1.** (A) Absorbance and (B) photoluminescence spectra of $Cs_{0.78}Pb_{1.11}Cl_3$ and $Mn^{2+}$-enriched $CsPbCl_3$ PNCs in toluene ($\lambda_{ex}$ = 350 nm) with inset of representative PNC solutions under a 365 nm UV lamp.

| Sample | Bandgap (nm) | Max $\lambda_{PL\ Host}$ (nm) | $FWHM_{Host}$ (nm) | Max $\lambda_{PL\ Mn}$ (nm) | $FWHM_{Mn}$ (nm) | Mn:Pb PL Peak ratio | Overall PLQY (%) |
|---|---|---|---|---|---|---|---|
| $Cs_{0.78}Pb_{1.11}Cl_3$ PNCs | 399 | 410 | 12 | | | | 0.5 ± 0.4 |
| $Cs_{0.75}Pb_{1.05}Mn_{0.07}Cl_3$ PNCs | 393 | 408 | 10 | 588 | 72 | 0.019:1 | 1.7 ± 0.6 |
| $Cs_{0.65}Pb_{0.91}Mn_{0.26}Cl_3$ PNCs | 396 | 406 | 11 | 586 | 74 | 0.057:1 | 7.7 ± 2.1 |
| $Cs_{0.56}Pb_{0.81}Mn_{0.41}Cl_3$ PNCs | 393 | 406 | 11 | 590 | 78 | 0.29:1 | 54 ± 8.4 |

**Table S1.** Photophysical data for $Cs_{0.83}Pb_{1.12}Cl_3$ and $Mn^{2+}$-enriched $CsPbCl_3$ PNCs. PL and PLQY were obtained using toluene as the solvent and blank and $\lambda_{ex}$ = 350 nm.

| Sample | Cs concentration (ppb) | Pb concentration (ppb) | Mn concentration (ppb) |
|---|---|---|---|
| $Cs_{0.78}Pb_{1.11}Cl_3$ PNCs | 130.3 | 287.5 | |
| $Cs_{0.75}Pb_{1.05}Mn_{0.07}Cl_3$ PNCs | 226.9 | 492.2 | 9.080 |
| $Cs_{0.65}Pb_{0.91}Mn_{0.26}Cl_3$ PNCs | 69.05 | 150.8 | 11.62 |
| $Cs_{0.56}Pb_{0.81}Mn_{0.41}Cl_3$ PNCs | 196.6 | 442.9 | 58.70 |

**Table S2.** ICP-MS concentrations for $Cs_{0.83}Pb_{1.12}Cl_3$ and $Mn^{2+}$-enriched $CsPbCl_3$ PNCs.

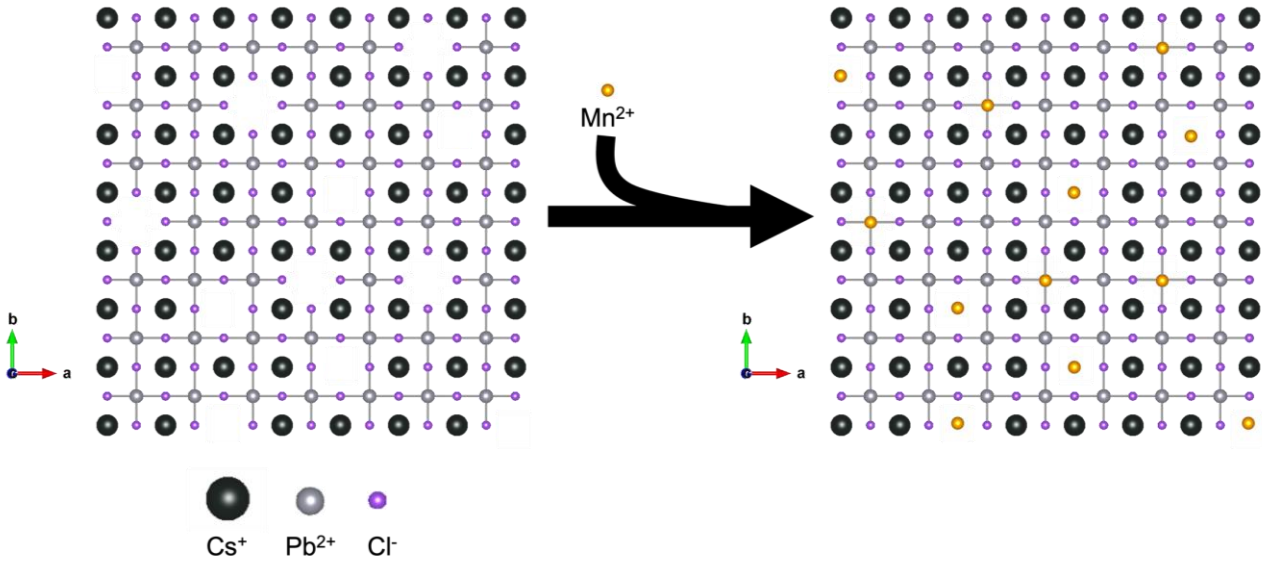


**Scheme S1.** Representation of $Mn^{2+}$ ions replacing the Cs+ and $Pb^{2+}$ vacancies within the crystal structure.

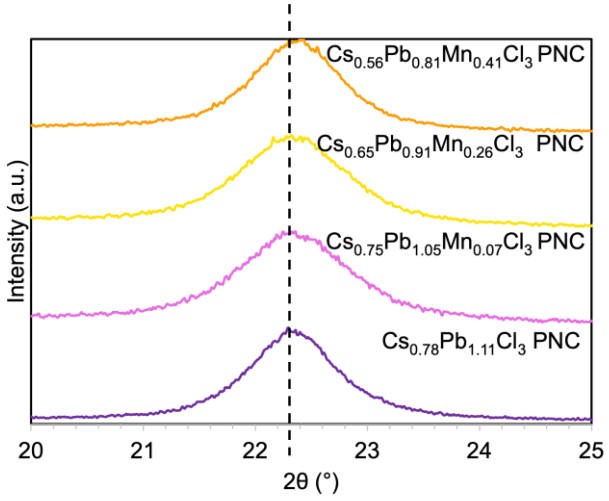


**Figure S2.** PXRD patterns of PNCs zoomed in at the 22 ° 2θ reflection to show the shift to higher angles. After the PNC synthesis, the centrifuged pellet was placed onto a zero background PXRD sample holder and left to run.

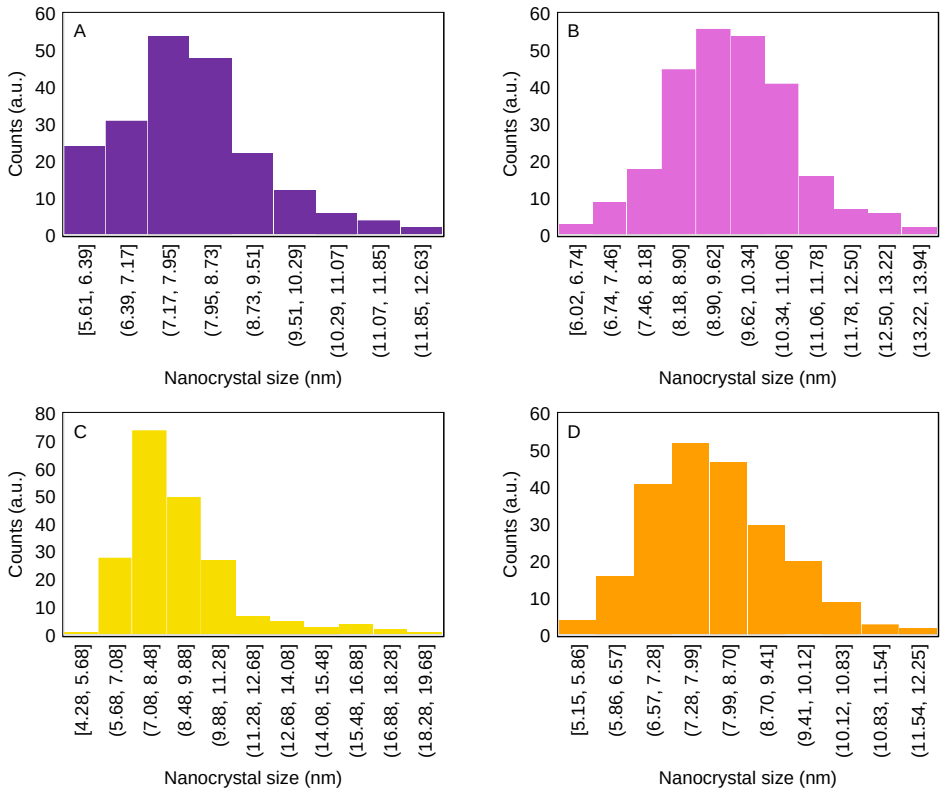


**Figure S3.** Size distribution for (A) $Cs_{0.78}Pb_{1.11}Cl_3$ PNCs, (B) $Cs_{0.75}Pb_{1.05}Mn_{0.07}Cl_3$ PNCs, (C) $Cs_{0.65}Pb_{0.91}Mn_{0.26}Cl_3$ PNCs, and (D) $Cs_{0.56}Pb_{0.81}Mn_{0.41}Cl_3$ PNCs using ~200 particles.

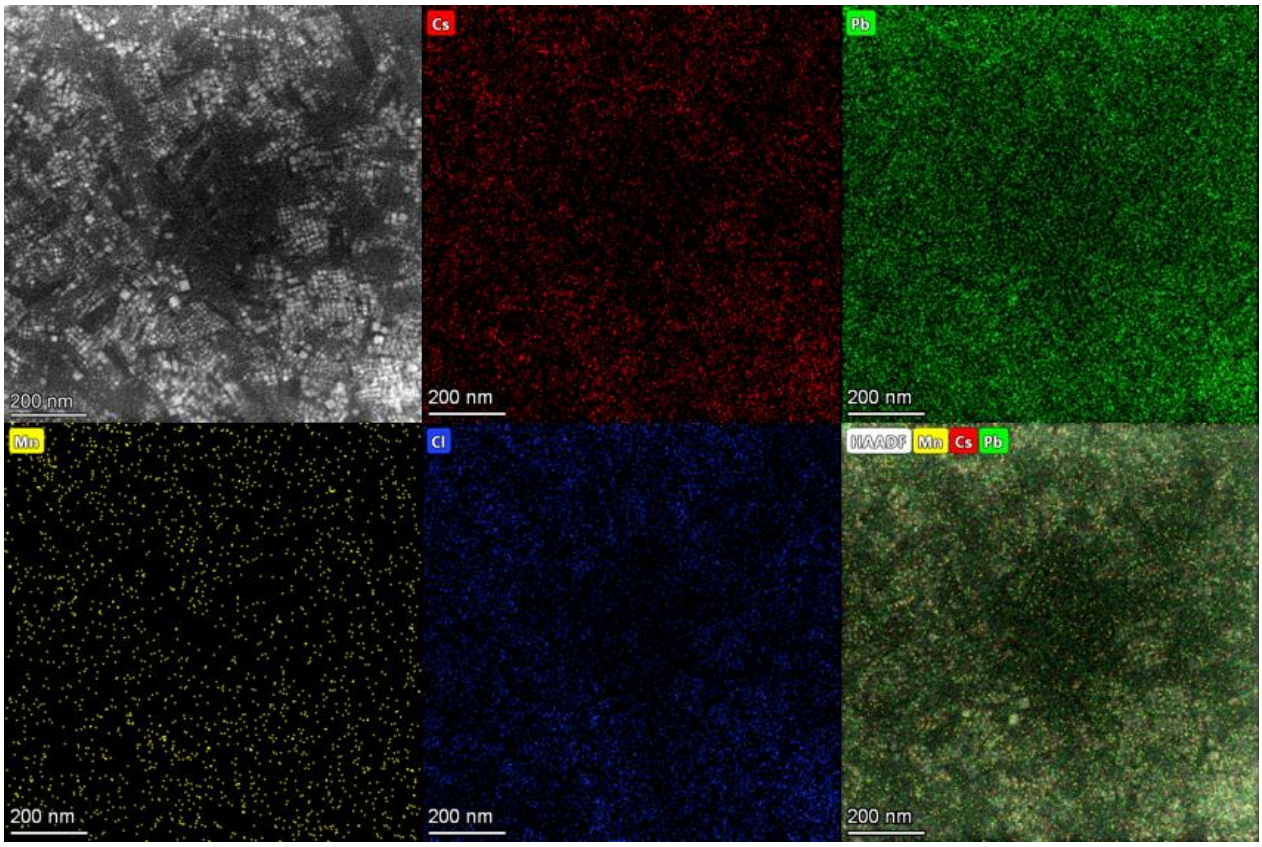


**Figure S4.** High-angle annular dark-field scanning TEM (HAADF-STEM) micrographs and EDS mapping of $Cs_{0.65}Pb_{0.91}Mn_{0.26}Cl_3$ PNCs (the PNC solution was diluted 50× in hexanes before being deposited onto the TEM grid).

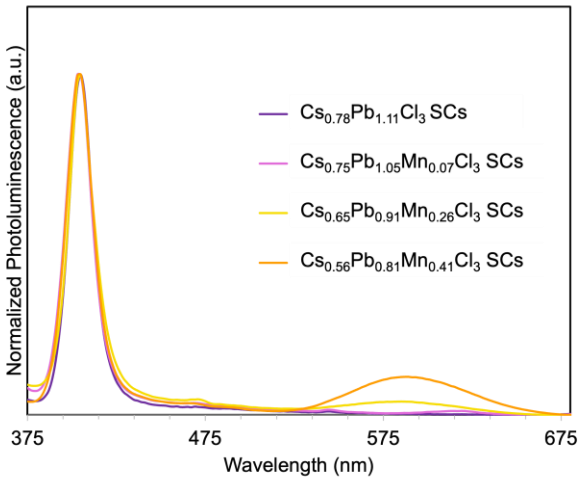


**Figure S5.** Photoluminescence spectra of $Cs_{0.78}Pb_{1.11}Cl_3$ and $Mn^{2+}$-enriched $CsPbCl_3$ SCs ($\lambda_{ex}$ = 350 nm).

| Sample | Max $\lambda_{PL\ Host}$ (nm) | $FWHM_{Host}$ (nm) | Max $\lambda_{PL\ Mn}$ (nm) | $FWHM_{Mn}$ (nm) | Mn:Pb PL Peak ratio | Overall PLQY (%) |
|---|---|---|---|---|---|---|
| $Cs_{0.78}Pb_{1.11}Cl_3$ SCs | 405 | 18 | | | | 0.23 ± 0.08 |
| $Cs_{0.75}Pb_{1.05}Mn_{0.07}Cl_3$ SCs | 403 | 18 | 543, 619 | 38, 36 | 0.012:1 | 0.53 ± 0.08 |
| $Cs_{0.65}Pb_{0.91}Mn_{0.26}Cl_3$ SCs | 405 | 20 | 585 | 83 | 0.039:1 | 2.4 ± 0.17 |
| $Cs_{0.56}Pb_{0.81}Mn_{0.41}Cl_3$ SCs | 405 | 20 | 588 | 84 | 0.11:1 | 11 ± 4.1 |

**Table S3.** Photophysical data for $Cs_{0.78}Pb_{1.11}Cl_3$ and $Mn^{2+}$-enriched $CsPbCl_3$ SCs. PL and PLQY were obtained using silicon substrates as the blank and $\lambda_{ex}$ = 350 nm.

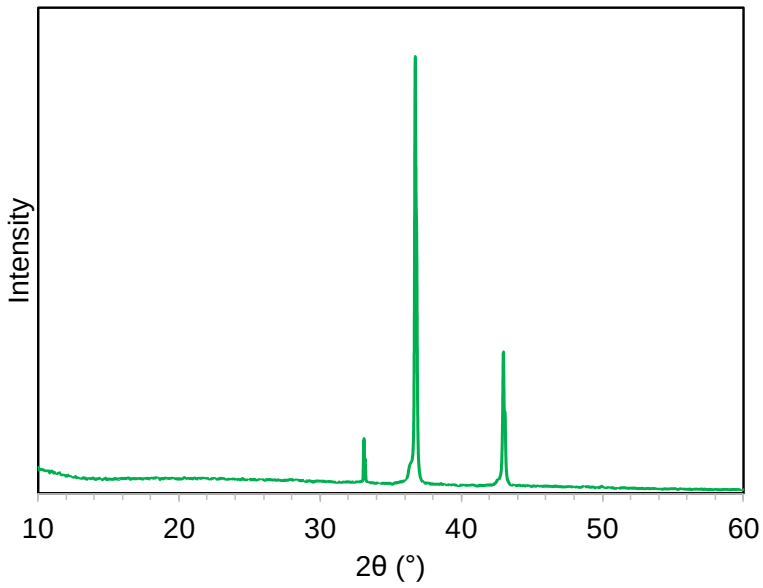


**Figure S6.** PXRD diffractogram of a blank silicon substrate that was used for the self-assembly of PNCs into SCs.

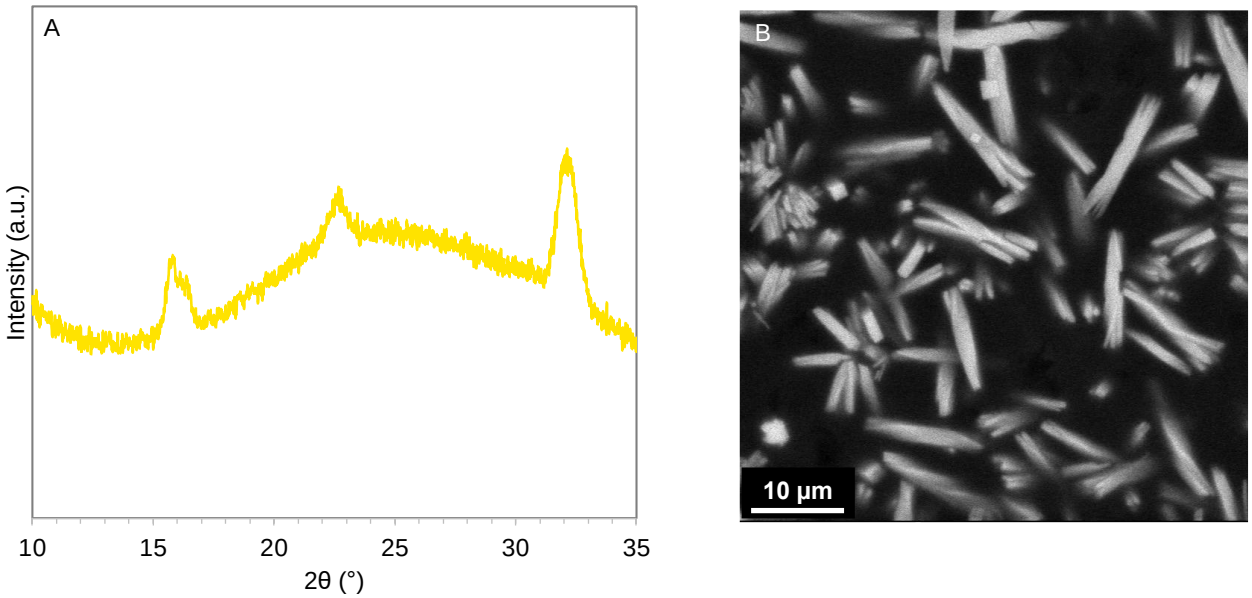


**Figure S7.** (A) PXRD pattern and (B) SEM micrograph of "$Cs_{0.65}Pb_{0.91}Mn_{0.26}Cl_3$" SCs using a different PNC batch demonstrating some rod-like superstructures instead of cubic structures reported in the main text. This demonstrates that the quality of the $Mn^{2+}$-enriched PNCs plays a large role within the self-assembly of the PNCs into SCs, and until the synthesis is completely optimized, some SC structural changes may occur.

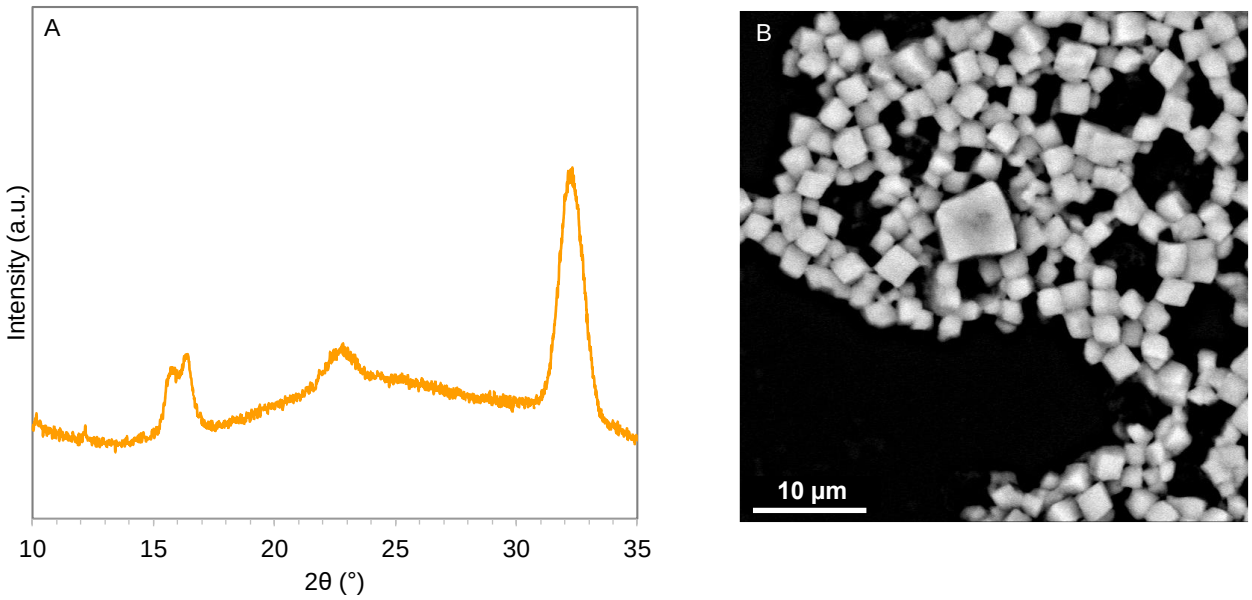


**Figure S8.** (A) PXRD pattern and (B) SEM micrograph of "$Cs_{0.56}Pb_{0.81}Mn_{0.41}Cl_3$" SCs using a different PNC batch demonstrating cubic superstructures instead of rod-like structures reported in the main text. This demonstrates that the quality of the $Mn^{2+}$-enriched PNCs plays a large role within the self-assembly of the PNCs into SCs, and until the synthesis is completely optimized, some SC structural changes may occur.

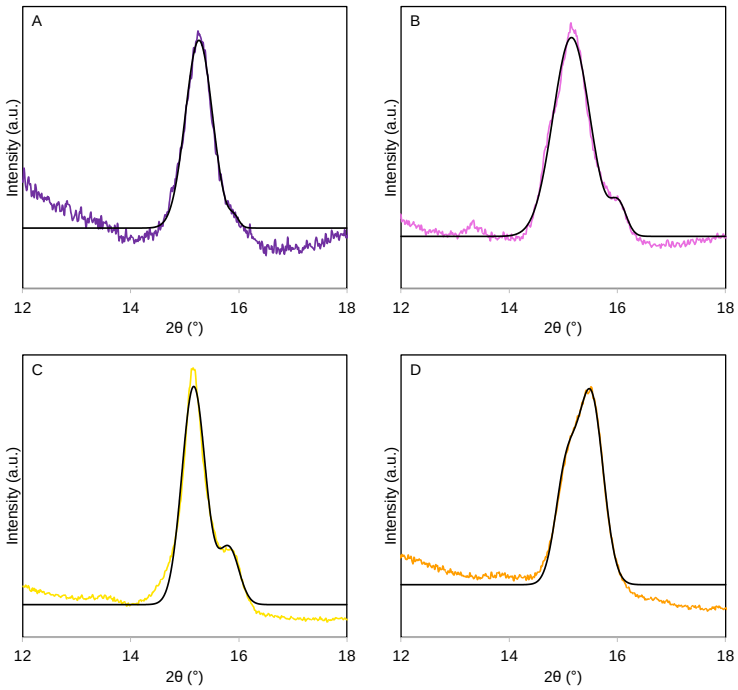


**Figure S9.** Gaussian fitting using Origin software of the PXRD patterns of (A) $Cs_{0.78}Pb_{1.11}Cl_3$ SCs, (B) $Cs_{0.75}Pb_{1.05}Mn_{0.07}Cl_3$ SCs, (C) $Cs_{0.65}Pb_{0.91}Mn_{0.26}Cl_3$ SCs, and (D) $Cs_{0.56}Pb_{0.81}Mn_{0.41}Cl_3$ SCs.

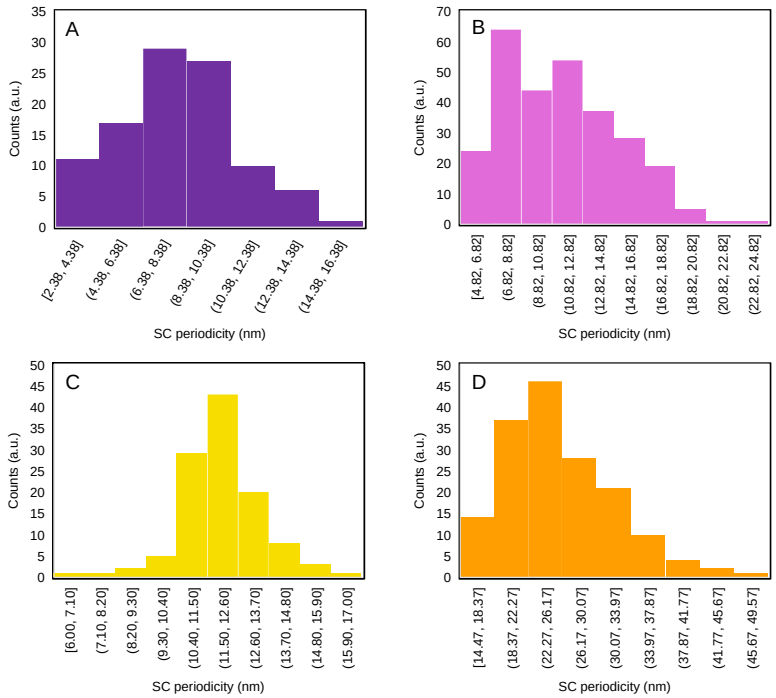


**Figure S10.** Distributions of SC periodicity measurements from TEM micrographs of (A) $Cs_{0.78}Pb_{1.11}Cl_3$ SCs, (B) $Cs_{0.75}Pb_{1.05}Mn_{0.07}Cl_3$ SCs, (C) $Cs_{0.65}Pb_{0.91}Mn_{0.26}Cl_3$ SCs, and (D) $Cs_{0.56}Pb_{0.81}Mn_{0.41}Cl_3$ SCs using ImageJ.

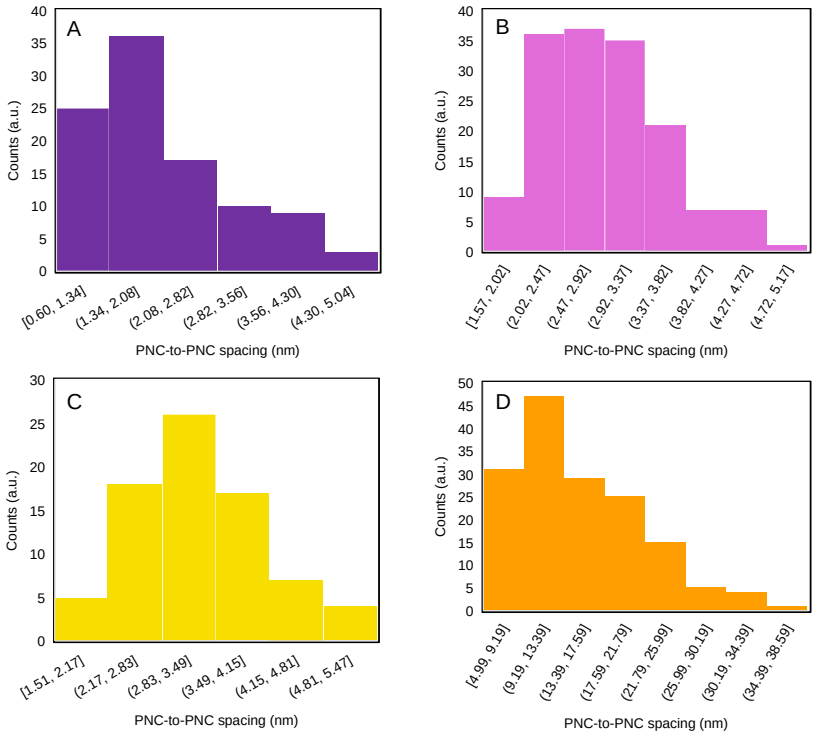


**Figure S11.** Distributions of PNC-to-PNC spacing measurements from TEM micrographs of (A) $Cs_{0.78}Pb_{1.11}Cl_3$ SCs, (B) $Cs_{0.75}Pb_{1.05}Mn_{0.07}Cl_3$ SCs, (C) $Cs_{0.65}Pb_{0.91}Mn_{0.26}Cl_3$ SCs, and (D) $Cs_{0.56}Pb_{0.81}Mn_{0.41}Cl_3$ SCs using ImageJ.

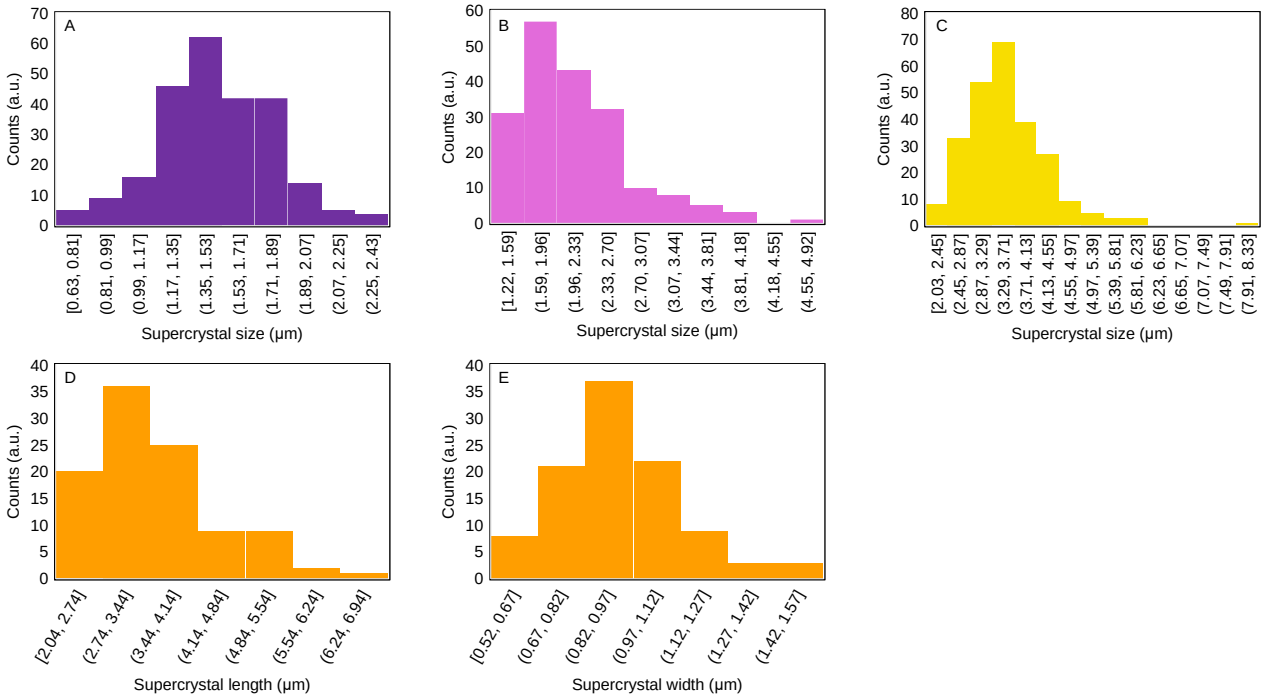


**Figure S12.** Size distribution of ((A) $Cs_{0.78}Pb_{1.11}Cl_3$ SCs, (B) $Cs_{0.75}Pb_{1.05}Mn_{0.07}Cl_3$ SCs, (C) $Cs_{0.65}Pb_{0.91}Mn_{0.26}Cl_3$ SCs, and (D-E) $Cs_{0.56}Pb_{0.81}Mn_{0.41}Cl_3$ SCs from SEM micrographs using ImageJ on ~100 particles.